

Experimental and CFD Modeling of Rubble Weir

Mohamed Ahmed¹, Mohamed Noureldin², Yehia Kamal², Hesham Nazmy³

¹(Master student, Irrigation & Hydraulics Dept. / Faculty of Engineering / Ain Shams University, Egypt)

²(Prof., Irrigation & Hydraulics Dept. / Faculty of Engineering / Ain Shams University, Egypt)

³(Ass. Prof., Irrigation & Hydraulics Dept. / Faculty of Engineering / Ain Shams University, Egypt)

Abstract: Experimental and numerical models were conducted to investigate water flow over gabion weirs. In the experimental study, the water surface profile (WSP) was measured for different discharges, flow patterns and downstream face slopes. In the numerical study, ANSYS® FLUENT Computational Fluid Dynamics (CFD) software was used to numerically simulate the flow over gabion weirs. The Reynolds-averaged Navier–Stokes equations were solved to predict the flow domain. The volume of fluid (VOF) method was applied to treat the complex free-surface flow. Structured high dense mesh was employed. The standard k-ε turbulence model was used to analyze turbulence downstream weir. The experimental results were used to verify the numerical model by two statistical indicators; the root mean square error (RMSE) and the mean absolute percent error (MAPE). Numerical results of the WSP showed good agreement with the experimental results. The values of RMSE and MAPE were between (0.60% – 2.49%) and (0.53% – 1.92%) respectively.

Key words: Gabions, Porous Weir, Experiment Model, CFD, VOF, Water Surface Profile.

Date of Submission: 22-06-2019

Date of acceptance: 05-07-2019

I. Introduction

Recycled agricultural and domestic drainage waters are considered among the most important available water resources. One of the methods adopted in the treatment of drainage water is the self-purification reactor (SPR) using the action of bacteria situated on rubble weirs installed across drains. For easy construction and maintenance, the rubble is filled in cages, known as “Gabions”. Bacteria inhabiting inside the gabion weir decomposes suspended organic matter, then gabions are periodically cleaned.

Since the 19th century, the hydraulic characteristics of weirs have been extremely studied with many experimental investigations such as **Bélanger 1841, 1849, Rouse, 1950, Bos, 1989 and Azimi&Rajaratnam 2009**. Most of the experimental works were oriented to understand the flow characteristics over weirs as well as the determination of the coefficients of discharge under free and submerged flow conditions (see **Fritz & Hager, 1998**). **Michioku et al. 2004, Hassan I. 2011, Leu et al. 2008 and Mohammed F. et al. 2015** studied the discharge through a permeable rubble mound weir and compared results with solid weirs.

Lately, several numerical studies were carried out to find the flow pattern around weirs. **Reda M, 2011**, and **Ghorban&Hadi, 2018** studied the flow over rectangular sharp-crested weirs using CFD modelling, and found agreement between measured results and computed CFD results. **Haun et al. 2011** compared results from two CFD codes; Flow-3D software, which uses the Volume of Fluid VOF method with a fixed grid, and SSIIM2 software, which uses an algorithm based on the continuity equation and the Marker-and-Cell method, together with an adaptive grid. The two codes were used to simulate water flow over a trapezoidal broad-crested weir. **Shaymaa et al. 2017** simulated water flow over broad crested weir and stepped weir with different turbulence models (Standard k-ε, RNG k-ε, Realizable k-ε, and Standard k- ω) using 2-D CFD code (FLUENT software). They reported that measured water surface profiles (WSP) were best matched by the standard k-ε model data and worst matched by the standard k-ω data. Also, the numerical results of stepped weir were more similar than broad crested weir. **Diao et al. 2018** studied the effect of the upstream angle on flow over a trapezoidal broad crested weir based on numerical simulations using OpenFOAM software. The statistical results for two turbulence models (standard k-ε model and the SST k-ω model) showed good agreement in terms of predicting the WSP. **Mohammadpour et al. 2013** simulated the WSP and the vertical velocity profile around gabion weirs using three variants of the k-ε and the RSM turbulence models. They showed that stream-wise velocities upstream porous weirs obtained from the standard k-ε turbulence models are better than those obtained from other turbulence models.

While many research works are found regarding the biological action of the SPR, limited data exists to evaluate the effect of geometric characteristics of the gabion weirs on the complex flow over them. In this study, the flow over gabion weirs is examined experimentally and using CFD 2-D numerical modeling technique. The fractional volume of fluid method (VOF) is employed to determine the free-surface and a structured mesh is used to generate the calculation domain. The material property of the porous medium is

simulated using the viscous resistance and inertial resistance parameters. Water surface profiles (WSP) obtained experimentally and numerically are compared.

II. Experimental Work

The experiments tests were carried out in the Hydraulic Engineering Laboratory, Ain shams University, Cairo, Egypt. The experiments were conducted in rectangular horizontal flume 245.0 cm long. It is a closed operating system and its sides are fabricated of 0.13 cm thickness clear Plexiglas, and has a cross section of 15.3 cm width and 30.0 cm depth. Near the end of the flume, there is a tailgate to regulate the water levels. Discharge is measured by a calibrated orifice meter. A hook depth gauge fixed to the measuring carriage was used to measure water surface profile with an accuracy of ± 0.01 cm.

The models of the rubble weirs were made from blocks of gabion laid to give three configurations. The dimensions of one block of the gabion were $(4.5 \times 5.1 \times 3.8)$ cm. As shown in Figure 1, the three configuration models (A, B, and C) have the same vertical face of the upstream (height 11.4 cm), and different downstream faces (vertical, stepped 1:1, and stepped 2:1), respectively. The weir length was the same as the flume width and the crest widths were (13.5, 9.0, and 4.5 cm), respectively.

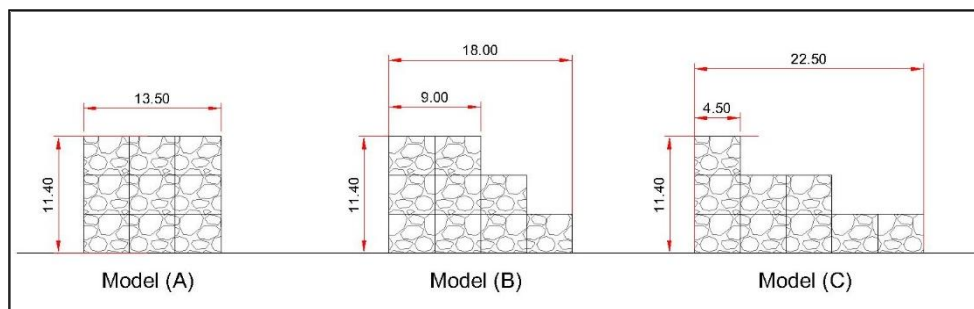
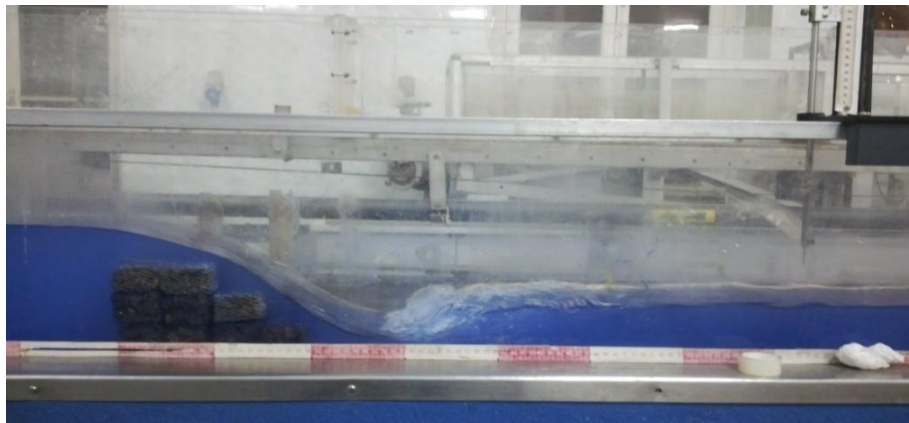


Figure 1: Definition sketch of models used in the experiments

The discharges examined were 1.5, 3.0, 4.5, 6.0, and $7.5 \text{ m}^3/\text{hr}$. Three flow patterns were examined:

- The free flow: The tailgate height was set to zero,
- Partially submerged weir flow: The tail water depth was set to a value less than the crest level, and
- Submerged weir flow: The tail water depth submerged completely the weir crest.

The total experimental runs were 45. WSPs were measured at sections upstream, over the gabion weirs, and downstream using a point gage with an accuracy of ± 0.01 cm. Picture 1 shows an example of the flow pattern over model (B) in case of partially submerged weir flow.



Picture 1: View of the flow pattern

III. Experimental Results

WSPs for the models having three configurations gabions and using the examined discharges are drawn in the longitudinal direction. Figures 2, 3 and 4 show the different water surface profiles for the models A, B, C for different discharges and flow cases. The distance X is measured from the flume entrance, and levels are measured from flume bed level.

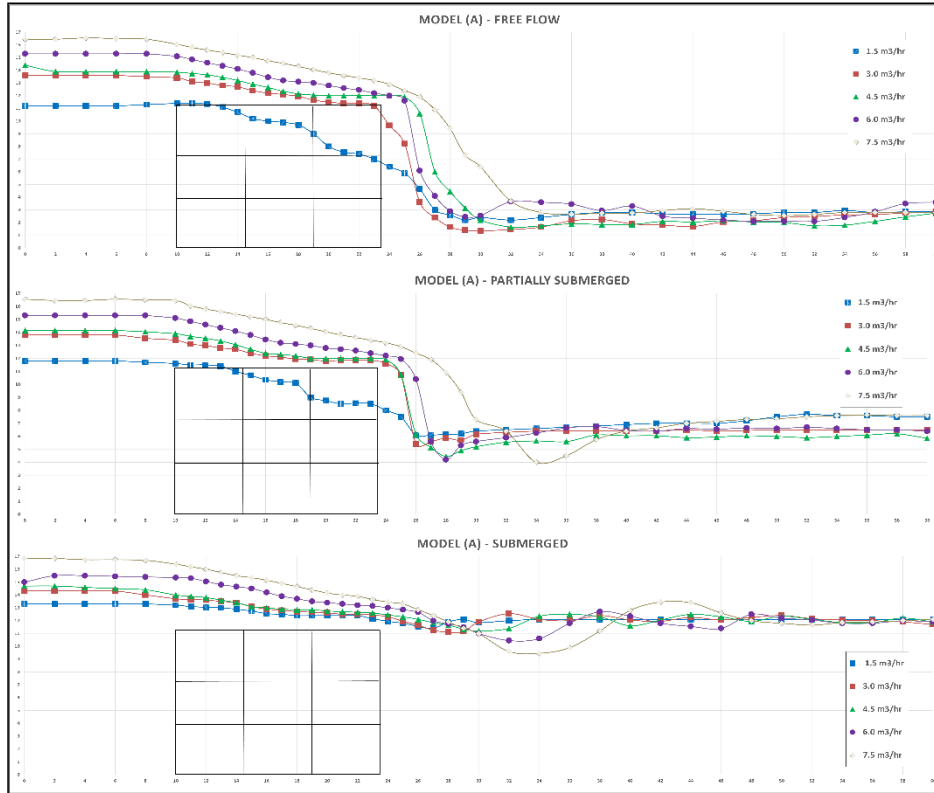


Figure 2: Water surface profile along the longitudinal side of the model (A)

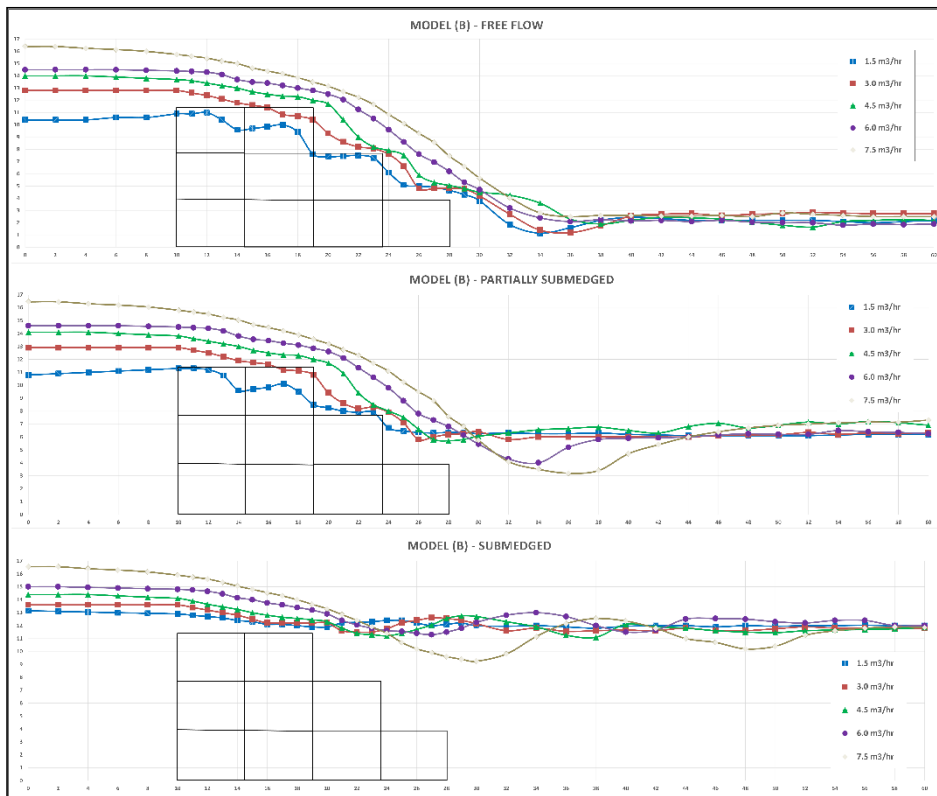


Figure 3: Water surface profile along the longitudinal side of the model (B)

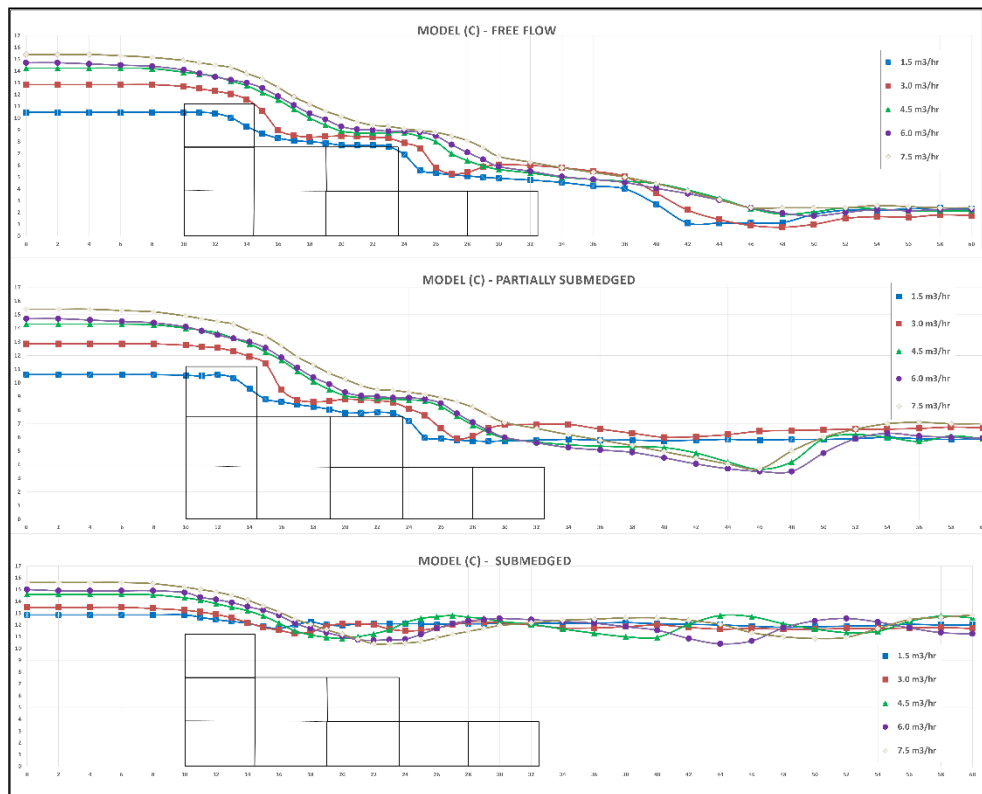


Figure 4: Water surface profile along the longitudinal side of the model (C)

IV. CFD Modelling

Computational Fluid Dynamics (CFD) is a branch of fluid mechanics that uses numerical computations and data structures to analyze and solve problems that involve fluid flows. In this study, numerical modeling was carried out using ANSYS® *FLUENT* (v.19.2 academic). *FLUENT* is one of CFD commercial software that has the capacity to solve 2-D and 3-D problems of open channel flow and the ability to predict flow profile over weirs.

1- Governing Equation

The Navier–Stokes equations are the fundamental basis of almost all CFD problems. These equations can be simplified by removing terms describing viscous actions to yield the Euler equations. Further simplification, by removing terms describing vorticity yields the full potential equations.

2- Numerical Schemes

The computational fluid dynamics package *FLUENT* was used to solve the non-linear and partial differential equations. Based on finite difference methods, *FLUENT* uses a control volume to solve the equations. To enable computations in a complex domain, the governing equations are discretized on grids using the implicit method. In this study, a first-order Power-Law scheme and a first order upwind scheme are used to interpolate the convection fluxes and momentum equation, respectively. A Semi-Implicit algorithm (SIMPLE) is employed to solve the equations with an iterative line-by-line matrix solver.

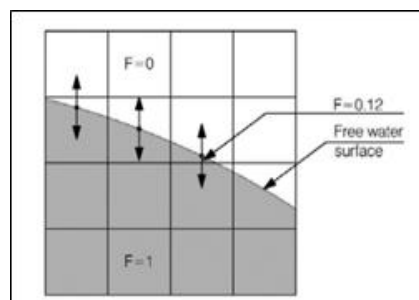
3- Turbulence Modeling

For quick solutions in the case of complex turbulent flows, the very fine mesh near the wall can be omitted, meaning that Reynolds stress models are able to provide better predictions. Examples of such flows are turbulent flows with high degrees of anisotropy, significant streamline curvature, flow separation, and zones of recirculation and influence of mean rotation effects. Reynolds stress models offer significantly better accuracy than eddy-viscosity based turbulence models, and is computationally cheaper than Direct Numerical Simulations (DNS) and Large Eddy Simulations (LES). $k-\omega$ model and $k-\epsilon$ model are two common two-equation turbulence models. $k-\omega$ model is used as a closure for the Reynolds-averaged Navier–Stokes equations (RANS). The model attempts to predict turbulence by two partial differential equations (PDEs) for two variables; the turbulence kinetic energy (k) and the specific rate of dissipation (ω). On the other hand, $k-\epsilon$ model gives a general description of turbulence by means of two transport PDEs. The original impetus for the $k-\epsilon$ model was to improve the mixing-length model, as well as to find an alternative to algebraically prescribing turbulent

length scales in moderate to high complexity flows. Generally, $k-\epsilon$ model is the most common model used to simulate mean flow characteristics for turbulent flow conditions, while $k-\omega$ model is capable of solving turbulence parameters very close to boundary or wall region with very fine meshing near to the wall. For a much more practical approach, the standard $k-\epsilon$ model is used in this study based on the best understanding of the relevant processes, thus minimizing unknowns and presenting a set of equations which can be applied to a large number of turbulent applications.

4- Free-Surface Modelling

The free water surface represents a particular challenge in 2-D and 3-D numerical models. Every selected computer program uses different method. *FLUENT* uses the Volume of Fluid Method (VOF). This is a two-phase approach where both water and air are modeled in the grid. The method is based on the concept that each cell has a fraction of water (F), which is given the number 1 when the element is totally filled with water and 0 when the element is filled with air. If the value is between 1 and 0, the element contains the free water surface. A transport equation is solved to model water surface in the absence of any inter-phase mass transfer which can be written as:



$$\frac{\partial F}{\partial t} + u \frac{\partial F}{\partial x} + v \frac{\partial F}{\partial y} = 0 \quad (1)$$

Where u and v are fluid velocity components in the x and y directions respectively.

5- Domain geometry and structured mesh

The geometry describes the shape of the problem to be analyzed. It can consist of volumes, faces (surfaces), edges (curves) and vertices (points). *FLUENT* can handle a number of different grid topologies. For this purpose, *DESIGNMODELER* is used to produce the geometry of the model. The geometry in the simulation domain was $100\text{cm} \times 25\text{cm}$. The distance from the inlet boundary to the weir is 40 cm , which exceeded 3 times the height of the weir to minimize the influence of the inlet boundary.

The mesh size is an important part of the numerical simulation because it affects not only the accuracy of the result but also the simulation time. To choose the optimum cell size, meshes with different dimension in edge and face are used. *FLUENT* uses meshes comprised of triangular or quadrilateral cells (or a combination of the two) in 2-D, and tetrahedral, hexahedral, polyhedral, pyramid, or wedge cells (or a combination of these) in 3-D. In this study, the mesh was 2-D structured with rectangular elements. Preliminary runs proved results to be independent of mesh size when there were at least 10469 nodes and 10122 elements. The mesh used in this study are shown in Figures 5, 6 and 7

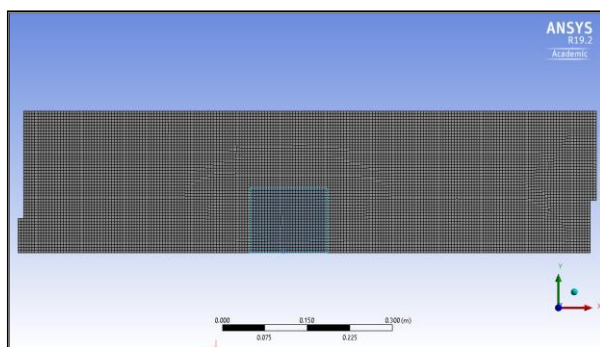


Figure 5: The mesh used for Model A

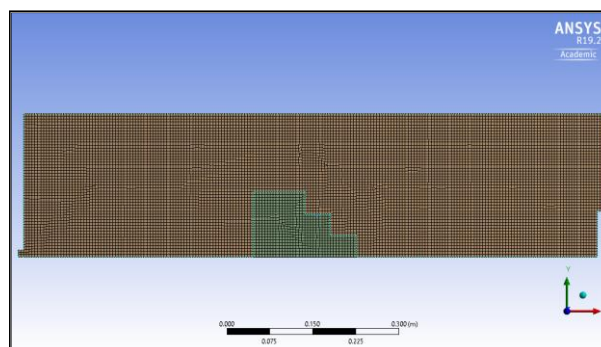


Figure 6: The mesh used for Model B

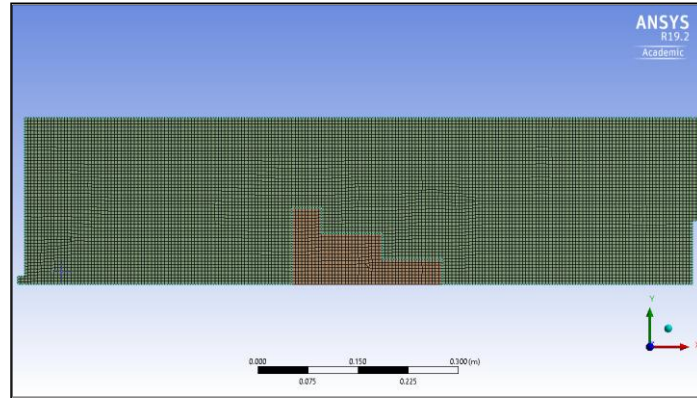


Figure 7: The mesh used for Model C

6- Boundary conditions

To have accurate results, appropriate conditions should be selected for boundaries based on the nature of the flow. In this study for numerical modeling of gabions, the boundary conditions imposed on the numerical domain were at the flume inlet and outlet, at the free surface, at the flume walls and porous media (refer to Figure 8).

In this study, a uniform distribution was given for all of the dependent variables at the inlet. The pressure outlet was specified at downstream of the channel. The water level is not defined at the outlet and is allowed to change in every simulation depending on simulation conditions. Zero normal gradients and velocity were applied by defining asymmetric boundary condition above the air at the top surface. The grid covers the whole flume, so the inflow would be distributed over the whole flume depth. At the solid boundary, the no-slip boundary was used to set the velocity equal to zero at the walls and solid boundaries. Empirical wall functions were used to estimate the effect of walls on the flow as a standard wall function. The wall and porous zone were selected as boundary conditions for solid and porous weir, respectively. Two different parameters, viscous resistance and inertial resistance were used to define the percentage of porosity to porous weirs.

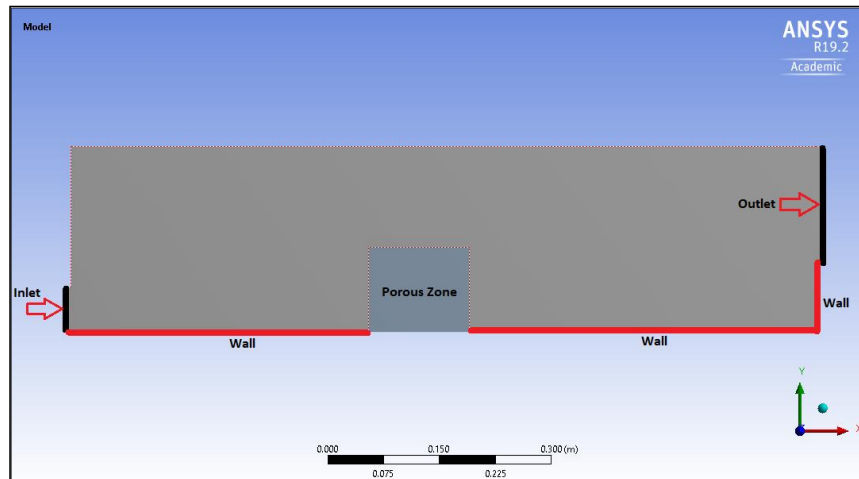


Figure 8: The boundary conditions using FLUENT

V. Verification of The CFD Model

The water surface profile over the models A, B, and C calculated by CFD and measured by experimental models are shown in Figures 9, 10, and 11, respectively. In figures, every color gives a pair of water surface profiles (WSP) data for the same flow parameters. Dotted line gives the measured WSP and the solid one gives the calculated WSP. Comparing the two water surface profiles, good match may be noticed. The differences may be due to assumptions adopted in the calculation of numerical WSP and difficulties in manually measuring the experimental WSP with the existence of high turbulence and air entrainment.

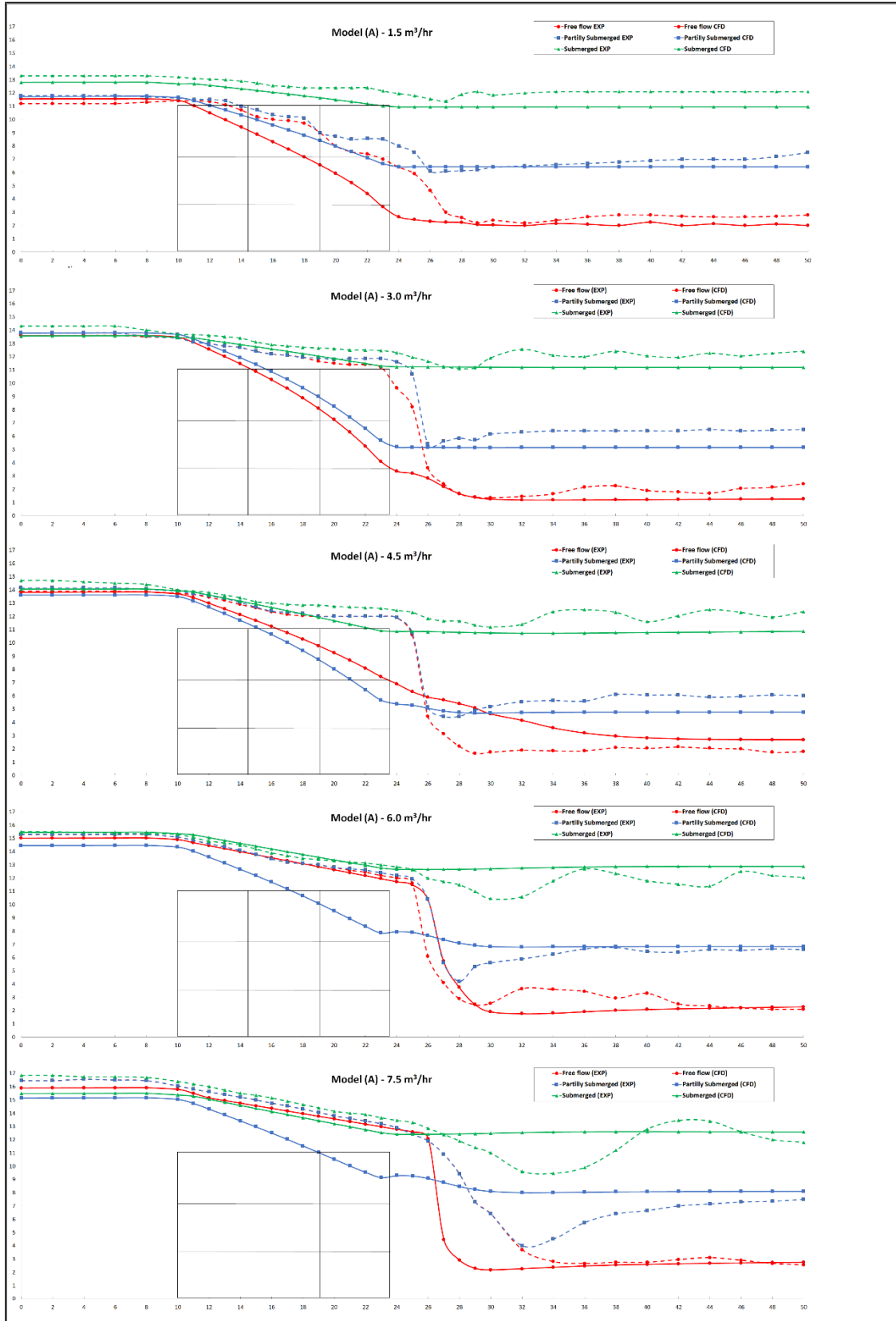


Figure 9: Comparison of water surface profile between experimental and CFD results for Model (A)

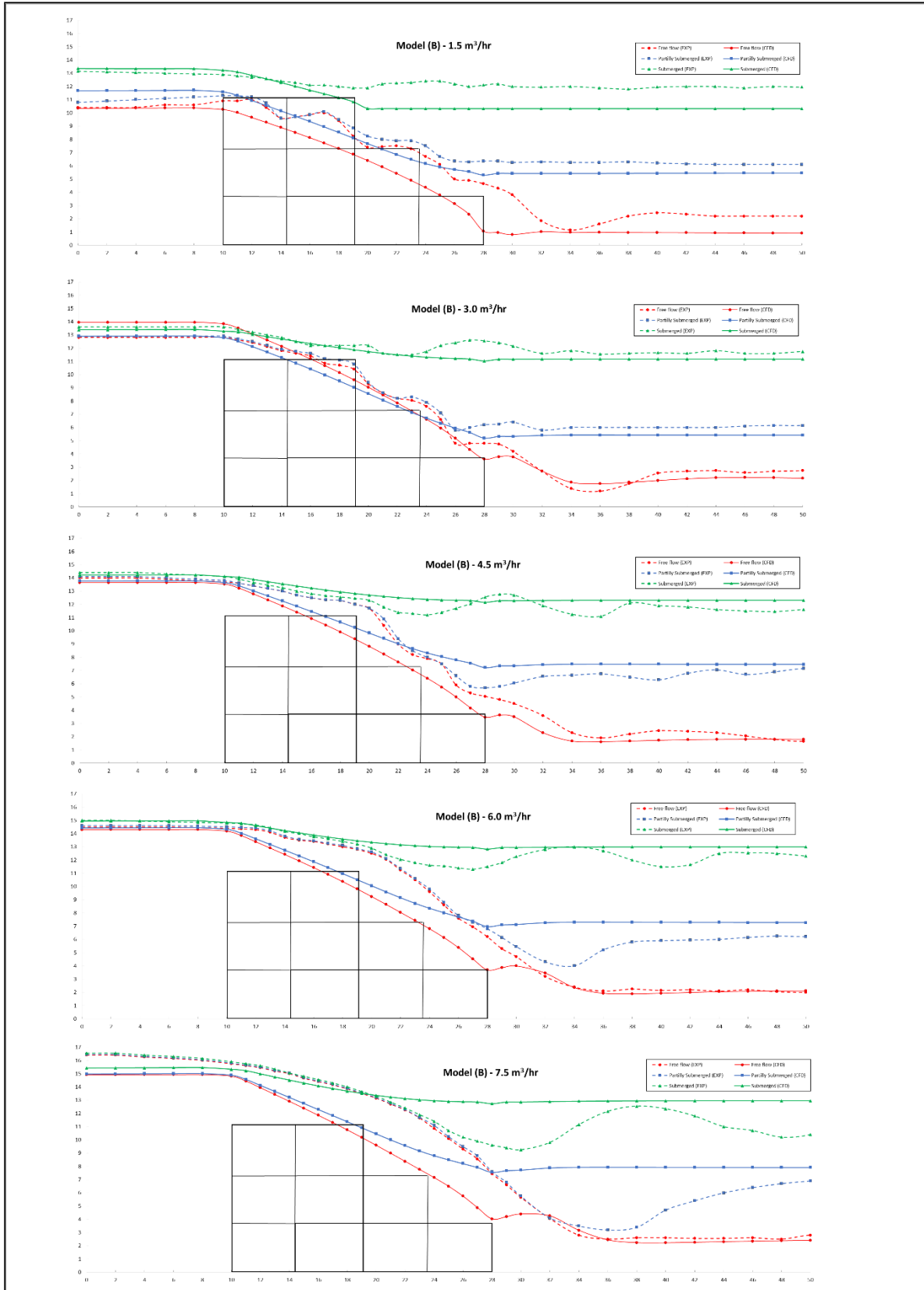


Figure 10: Comparison of water surface profile between experimental and CFD results for Model (B)

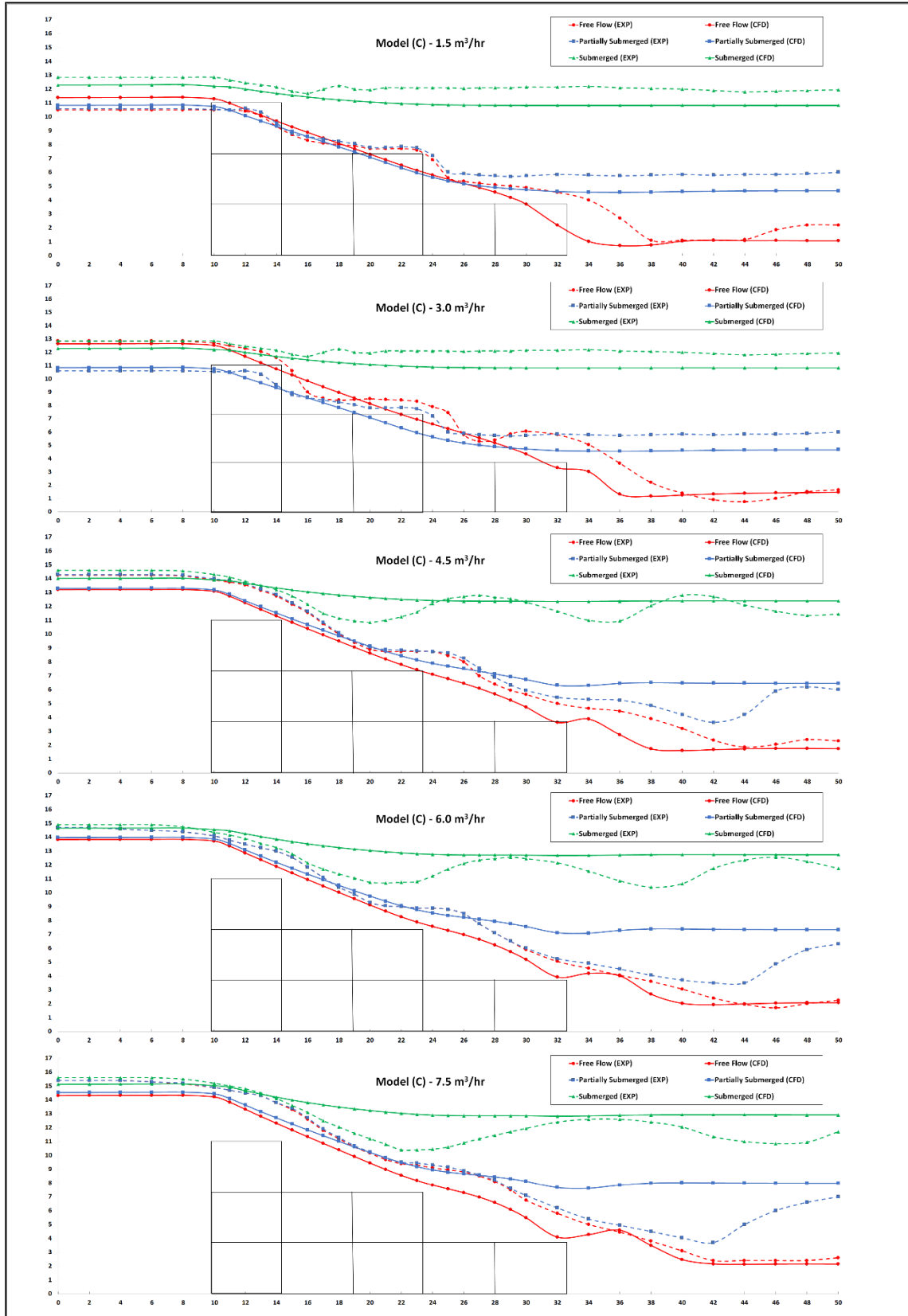


Figure 11: Comparison of watersurface profile between experimental and CFD results for Model (C)

To further verify the reliability of the numerical simulation, two statistical indicators, the root mean square error (RMSE) and the mean absolute percent error (MAPE) are used to evaluate the accuracy of the numerical results. Both the RMSE and the MAPE must be small to ensure a good agreement between the

numerical and experimental results. The calculated values of the statistical indicators for the WSPs in the upstream, over weir, and downstream are listed in **Table 1**. As can be seen from **Table 1**, the values of RMSE and MAPE for the model (A) are between (0.77% – 2.49%), (0.53% – 1.88%) respectively, the values of RMSE and MAPE for the model (B) are between (0.60% – 2.21%), (0.46% – 1.92%) respectively, and the values of RMSE and MAPE for the model (C) are between (0.77% – 1.55%), (0.64% – 1.20%) respectively. Statistical results show that three models show good agreement between the measured and calculated WSP.

Table 1: The calculated Values of RMSE & MAPE for Water Surface Profiles

| Model | Flow Type | Q m ³ /hr | RMSE % | | | | MAPE % | | | |
|-------|---------------------|-------------------------|--------|------|------|-------------|--------|------|------|-------------|
| | | | U.S | Weir | D.S | Total | U.S | Weir | D.S | Total |
| (A) | Free Flow | 1.5 | 0.32 | 2.35 | 0.62 | 1.55 | 0.29 | 2.14 | 0.58 | 1.16 |
| | | 3.0 | 0.05 | 3.83 | 0.91 | 2.49 | 0.03 | 3.10 | 0.76 | 1.57 |
| | | 4.5 | 0.08 | 2.66 | 1.65 | 2.03 | 0.07 | 2.18 | 1.28 | 1.48 |
| | | 6.0 | 0.27 | 1.08 | 0.98 | 0.95 | 0.27 | 0.40 | 0.76 | 0.53 |
| | | 7.5 | 0.54 | 0.33 | 2.56 | 1.79 | 0.52 | 0.31 | 1.34 | 0.84 |
| | Partially Submerged | 1.5 | 0.06 | 1.00 | 0.73 | 0.79 | 0.06 | 0.89 | 0.61 | 0.63 |
| | | 3.0 | 0.15 | 3.46 | 1.20 | 2.33 | 0.09 | 2.66 | 1.17 | 1.60 |
| | | 4.5 | 0.50 | 3.66 | 1.06 | 2.43 | 0.50 | 3.01 | 0.99 | 1.72 |
| | | 6.0 | 0.82 | 2.90 | 0.97 | 1.98 | 0.82 | 2.63 | 0.66 | 1.48 |
| | | 7.5 | 1.28 | 2.81 | 1.67 | 2.17 | 1.28 | 2.66 | 1.34 | 1.88 |
| | Submerged Weir | 1.5 | 0.49 | 0.77 | 1.09 | 0.90 | 0.49 | 0.73 | 1.07 | 0.85 |
| | | 3.0 | 0.64 | 0.66 | 0.87 | 0.77 | 0.61 | 0.60 | 0.78 | 0.69 |
| | | 4.5 | 0.49 | 0.98 | 1.19 | 1.03 | 0.44 | 0.80 | 1.13 | 0.90 |
| | | 6.0 | 0.07 | 0.26 | 1.21 | 0.84 | 0.06 | 0.21 | 1.09 | 0.59 |
| | | 7.5 | 1.25 | 0.97 | 1.38 | 1.23 | 1.24 | 0.95 | 1.05 | 1.05 |
| (B) | Free Flow | 1.5 | 0.29 | 2.03 | 1.37 | 1.63 | 0.20 | 1.87 | 1.25 | 1.39 |
| | | 3.0 | 1.13 | 0.63 | 0.55 | 0.70 | 1.13 | 0.55 | 0.51 | 0.62 |
| | | 4.5 | 0.29 | 1.63 | 0.61 | 1.19 | 0.28 | 1.50 | 0.52 | 0.94 |
| | | 6.0 | 0.19 | 2.37 | 0.26 | 1.64 | 0.19 | 2.21 | 0.20 | 1.16 |
| | | 7.5 | 1.27 | 3.06 | 0.39 | 2.18 | 1.25 | 2.94 | 0.27 | 1.69 |
| | Partially Submerged | 1.5 | 0.66 | 0.82 | 0.74 | 0.77 | 0.63 | 0.72 | 0.74 | 0.71 |
| | | 3.0 | 0.05 | 0.94 | 0.72 | 0.78 | 0.02 | 0.84 | 0.70 | 0.66 |
| | | 4.5 | 0.26 | 1.16 | 0.75 | 0.93 | 0.25 | 1.01 | 0.69 | 0.78 |
| | | 6.0 | 0.17 | 1.55 | 1.62 | 1.47 | 0.17 | 1.32 | 1.46 | 1.21 |
| | | 7.5 | 1.25 | 2.01 | 2.61 | 2.21 | 1.23 | 1.86 | 2.17 | 1.92 |
| | Submerged Weir | 1.5 | 0.31 | 1.42 | 1.65 | 1.41 | 0.30 | 1.19 | 1.65 | 1.23 |
| | | 3.0 | 0.23 | 0.43 | 0.58 | 0.60 | 0.22 | 0.28 | 0.56 | 0.46 |
| | | 4.5 | 0.13 | 0.66 | 0.67 | 0.60 | 0.11 | 0.57 | 0.62 | 0.51 |
| | | 6.0 | 0.06 | 0.81 | 0.79 | 0.80 | 0.05 | 0.57 | 0.69 | 0.59 |
| | | 7.5 | 0.91 | 1.08 | 1.93 | 1.68 | 0.89 | 0.80 | 1.70 | 1.35 |
| (C) | Free Flow | 1.5 | 0.88 | 1.10 | 1.07 | 1.02 | 0.88 | 0.79 | 0.90 | 0.80 |
| | | 3.0 | 0.21 | 1.15 | 0.76 | 0.90 | 0.21 | 0.94 | 0.47 | 0.66 |
| | | 4.5 | 0.99 | 1.13 | 0.98 | 1.05 | 0.98 | 1.05 | 0.77 | 0.95 |
| | | 6.0 | 0.70 | 0.88 | 0.45 | 0.77 | 0.68 | 0.79 | 0.33 | 0.65 |
| | | 7.5 | 0.96 | 1.19 | 0.36 | 1.00 | 0.95 | 1.13 | 0.34 | 0.89 |
| | Partially Submerged | 1.5 | 0.24 | 0.92 | 1.21 | 0.95 | 0.23 | 0.78 | 1.21 | 0.82 |
| | | 3.0 | 0.34 | 0.91 | 1.14 | 0.93 | 0.34 | 0.81 | 1.12 | 0.83 |
| | | 4.5 | 0.95 | 0.82 | 1.39 | 1.05 | 0.95 | 0.71 | 1.12 | 0.87 |
| | | 6.0 | 0.56 | 1.02 | 2.48 | 1.55 | 0.54 | 0.73 | 2.23 | 1.12 |
| | | 7.5 | 0.75 | 1.01 | 2.41 | 1.52 | 0.74 | 0.72 | 2.07 | 1.09 |
| | Submerged Weir | 1.5 | 0.57 | 1.02 | 1.15 | 1.00 | 0.57 | 0.96 | 1.14 | 0.95 |
| | | 3.0 | 0.61 | 1.35 | 1.57 | 1.33 | 0.61 | 1.19 | 1.57 | 1.20 |
| | | 4.5 | 0.53 | 0.98 | 0.69 | 0.82 | 0.52 | 0.75 | 0.57 | 0.64 |
| | | 6.0 | 0.22 | 1.36 | 1.30 | 1.24 | 0.21 | 1.14 | 1.11 | 0.99 |
| | | 7.5 | 0.41 | 1.51 | 1.18 | 1.33 | 0.39 | 1.22 | 0.96 | 1.04 |

VI. Conclusion

The technique of CFD was used to model the case of flow over gabion weir in the three cases of flow over weir; free flow, partially submerged weir, and totally submerged weir. Within the limitations tested, the following can be concluded:

- The water surface profile for flow over gabion weir computed using CFD technique matches well with that measured in the laboratory experiments. This tells that the CFD may be used to simulate such flow.
- In this case of no high turbulence near the boundary, the use of k- ε model proved high ability in modeling the flow.

- The effect of mesh size on the results accuracy vanishes when the mesh size is at least 10469 nodes and 10122 elements.

References

- [1]. Horton, R.E.; Murphy, E.C. Weir Experiments, Coefficients, and Formulas; US Government Printing Office: Washington, DC, USA, 1906
- [2]. Azimi, A.H.; Rajaratnam, N.; Zhu, D.Z. Discharge Characteristics of Weirs of Finite Crest Length with Upstream and Downstream Ramps. *J. Irrig. Drain. Eng.* 2013, 139, 75–83.
- [3]. Azimi AH, Rajaratnam N (2009). Discharge characteristics of weirs of finite crest length. *Journal of Hydraulic Engineering* 135(12):1081–1085.
- [4]. Duguay, J.M.; Lacey, R.W.J.; Gaucher, J. A case study of a pool and weir fishway modeled with OpenFOAM and FLOW-3D. *Ecol. Eng.* 2017, 103, 31–42.
- [5]. Chen, Y.; Fu, Z.; Chen, Q.; Cui, Z. Discharge Coefficient of Rectangular Short-Crested Weir with Varying Slope Coefficients. *Water* 2018, 10, 204.
- [6]. Lei Jiang, Mingjun Diao *, Haomiao Sun and Yu Ren Numerical Modeling of Flow Over a Rectangular Broad-Crested Weir with a Sloped Upstream Face *Water* 2018, 10, 1663; doi:10.3390/w10111663
- [7]. Reza Mohammadpour a,†, Aminuddin Ab. Ghani a, Hazi Mohammad Azamathulla Numerical modeling of 3-D flow on porous broad crested weirs, *37* (2013) 9324–9337
- [8]. H.C. Chan, Y. Zhang, J.M. Leu, Y.S. Chen, Numerical calculation of turbulent channel flow with porous ribs, *J. Mech.* 26 (2010) 15–28.
- [9]. B. Dargahi, Experimental study and 3D numerical simulations for a free-overflow spillway, *J. Hydraul. Eng.* 132 (9) (2006) 899–907.
- [10]. F. Dias, J.B. Keller, J.M. Vanden-Broeck, Flows over rectangular weirs, *Phys. Fluids*
- [11]. Dr. Shaymaa A. M. Al-Hashimi. Experimental And Numerical Simulation Of Flow Over Broad Crested Weir And Stepped Weir Using Different Turbulence Models, *Journal of Engineering and Sustainable Development* Vol. 21, No. 02, March 2017
- [12]. Williams JJR (2007). Free-surface simulations using an interface-tracking finite volume method with 3D mesh movement. *Engineering Applications of Computational Fluid Mechanics* 1(1):49–56.
- [13]. Stefan Haun*, Nils Reidar B. Olsen and Robert Feurich Numerical Modeling of Flow Over Trapezoidal Broad-Crested Weir, *Engineering Applications of Computational Fluid Mechanics* Vol. 5, No. 3, pp. 397–405 (2011)
- [14]. Ghorban Mahtabi. Experimental and numerical analysis of flow over a rectangular full-width sharp-crested weir, *Water Science and Engineering* 2018, 11(1): 75e80
- [15]. S. Maeno, K. Michioku, S. Morinaga and T. Ohnishi. Hydraulic characteristics of a rubble mound weir and its failure process
- [16]. Michioku K., Fukuoka T. and Furusawa T. 2001. Permeability of a rubble mound weir, *Annual Journal of Hydraulic Engineering, JSCE*. Vol.45. 391-396.

Mohamed Ahmed. “Experimental and CFD Modeling of Rubble Weir.” *IOSR Journal of Mechanical and Civil Engineering (IOSR-JMCE)* , vol. 16, no. 4, 2019, pp. 17-27.